

Attenuation Distance of Low Frequency Waves Upstream of the Pre-Dawn Bow Shock:

GEOTAIL and ISEE3 Comparison

T. Sugiyama¹, T. Terasawa¹, H. Kawano¹, T. Yamamoto², S. Kokubun³, L. A. Frank⁴,
K. Ackerson⁴, and R. T. Tsurutani⁵

Received _____; accepted _____

to be submitted to the *Geophysical Research Letters*, 1994,

Short title: BOW SHOCK UPSTREAM WAVES

¹DEPP, the University of Tokyo, Tokyo, Japan

²ISAS, Kanagawa, Japan

³STEL, Nagoya University, Toyokawa, Japan

⁴Dept. of Physics and Astronomy, the University of Iowa, Iowa

⁵Jet Propulsion Laboratory, California Institute of Technology

Introduction.

The low frequency ($<$ proton Larmor frequency) shock upstream waves have been studied extensively in the context of the wide-spread dissipation process at the quasi-parallel shock [Fairfield, 1969; Hoppe *et al.*, 1981; Le and Russell, 1992 and references therein]. At the shock front, suprathermal ions ($>$ several keV) are injected upstream by the specular reflection process [Paschmann *et al.*, 1980] and/or the process intrinsically related to the shock formation process itself [H $\&$ *et al.*, 1990; Scholer and Burgess, 1992]. These ions then excite low frequency magnetic waves through the ion-ion beam cyclotron instability [Barnes, 1970; Watanabe and Terasawa, 1981; Winske and Leroy, 1985]. Extensive studies of these wave and ion properties, however, have been made mainly for the upstream region of $X > -10$ Re, and the study of upstream region of $X < -10$ Re is quite limited. In this letter, we present the result of statistical study of wave amplitude distribution in the wide region of $-50 < X < 15$ Re, utilizing the magnetic field data from both ISEE-3 and GEOTAIL spacecraft,

Observations.

Figure 1 shows the orbits of these two spacecraft projected onto the GSE (geocentric solar ecliptic) XY and XZ planes. A dashed curve in Fig. 1 shows the nominal shock location [Fairfield, 1971]. (Average solar wind aberration is assumed to be 40.) The ISEE-3 spacecraft traveled the upstream region of the pre-dawn bow shock during the period of 24-30 September, 1983. Terasawa *et al.* [1985] discussed the properties of energetic ions (>30 keV) observed during this upstream interval, and concluded that the acceleration of these ions mainly occurs in the near-earth upstream region, and that the particle acceleration at the distant bow shock is weak. In this paper, we study the

We observe in Fig. 5a and 5b that the wave amplitudes show dependence on X_s , increasing toward the shock subsolar point (at $X_s \sim 14$ Re), Fig. 5c shows the distance D along the IMF line from the nominal shock surface to the spacecraft, which we expect to be another controlling factor of the wave intensity. Since GEOTAIL was close to the bow shock, the dataset seems to have included large amplitude waves within the shock ramp region. In Fig. 5b, the nominal upstream intervals (open circles for 45 intervals) are discriminated from the near-shock intervals (dots for 20 intervals), within 30 min of which GEOTAIL crossed the bow shock. Solid curves in Figure 5a and 5b are the results of the least-square fitting of the functioned form of $A \exp(X_s/L_X - D/L_D)$ to the combined data sets of ISPE 3/G EOTAIL observations, where the near-shock intervals for G EOTAIL were omitted. The attenuation distances are $L_X = 545 - 9 \text{ Re}$

and $L_D = 51 \pm 32 R_E$ with $A = 0.404 \pm 0.04$. Accounting the difference in numbers of 5 ruin intervals, we have set the statistical weights of ISEE-3 and GEOTAIL with a ratio of 1:4. The above statistical result shows $L_X \sim L_D$. Including the GEOTAIL near-shock data, we obtain $L_X = 554.10 R_E$ and $L_D = 36 \pm 15 R_E$ with $A = 0.43 \pm 0.04$ (dashed curves in Fig. 5a and 5b). In this calculation L_D is significantly smaller than L_X . However, L_D seems to be underestimated here owing to the contamination of data within the shock-ramp region.

Discussion.

We have compared the upstream wave observations from ISEE-3 and GIN-WAIL, whose acquisition times were separated over a decade. For such a comparison to be possible, we should have a similar solar wind condition. The basic solar wind parameters are tabulated in Table 1a and 1b [Rame *et al.*, 1978; Frank *et al.*, 1994]. As seen in the tables, the solar wind conditions were not completely identical: The Alfvén Mach numbers M_A in the GEOTAIL period were generally larger than those in the ISEE-3 period. (Note that this difference in M_A is mainly caused by the higher number densities in the latter period than the former. The ranges of the solar wind velocity themselves overlapped, and were within the nominal variation width.) Under the high M_A condition the bow shock surface is expected to shrink behind the nominal position, so that the actual field-aligned distance D for GEOTAIL would be larger than that shown in Fig. 5c. The underestimation of D for GEOTAIL might have led us to overestimate the attenuation distance L_D . However, the fact that we observed bow shock crossings on Aug. 7 indicates that the effect of high M_A on the shock position was not substantial. For complete discussion, we should use the fast magnetosonic Mach number M_F instead of M_A . Unfortunately, M_F for the ISEE-3 period is not available, since the ion temperature was not known. For the further refinement of the estimation of L_D and L_X , we are awaiting the compilation of the dataset from the another GEOTAIL orbit in the

References

- Bame, S. J., J. R. Asbridge, H. E. Felthouser, J. P. Glore, H. L. Hawk, and J. Chavez, ISEE-C solar wind plasma experiment, *IEEE Trans. Geosci. Electr.*, **GE-16**, 160, 1978.
- Barnes, A., Theory of generation of bow-shock-associated hydromagnetic waves in the upstream interplanetary medium, *Cosmic Electrodyn.*, **1**, 90, 1970.
- Fairfield, D. H., Bow shock associated waves observed in the far upstream interplanetary medium, *J. Geophys. Res.*, **74**, 3541-3553, 1969.
- Fairfield, D. H., Average and unusual locations of the earth's magnetopause and bow shock, *J. Geophys. Res.*, **76**, 6700-6711, 1971.
- Frandsen, A. M. A., B. V. Connor, J. van Amerfoort, and E. J. Smith, The ISEE-C vector helium magnetometer, *IEEE Trans. Geosci. Electron.*, **GE-16**, 195, 1978.
- Frank, L. A., K. L. Ackerson, W. R. Paterson, J. A. Lee, M. R. English, and G. L. Pickett, The comprehensive plasma instrumentation (CPI) for the GEOTAIL spacecraft, *J. Geomag. Geoelectr.*, **46**, 23-37, 1994.
- Hoppe, M. M., C. T. Russell, L. A. Wink, "I. F. Eastman, and E. W. Greenstadt, Upstream hydromagnetic waves and their association with backstreaming ion populations: ISEE 1 and 2 observations, *J. Geophys. Res.*, **86**, 4471-4482, 1981.
- Kokubun, S., T. Yamamoto, M. H. Acuña, K. Hayashi, K. Shiokawa, and H. Kawano, The GEOTAIL magnetic field experiment, *J. Geomag. Geoelectr.*, **46**, 7-21, 1994.
- Le, G., and C. T. Russell, A study of ULF wave foreshock morphology - II: Spatial variation of ULF waves, *Planet. Space Sci.*, **40**, 1215-1225, 1992.
- Mitchell, D. G., E. C. Roelof, T. R. Sanderson, R. Reinhard, and K.-P. Wenzel, ISEE/IMP observations of simultaneous upstream ion events *J. Geophys. Res.*, **88**, 5635-6644, 1983,
- Paschmann, G., N. Sckopke, J. R. Asbridge, S. J. Bame, and J. T. Gosling, Energization of solar wind ions by reflection from the earth's bow shock, *J. Geophys. Res.*, **85**, 4689-4693, 1980.
- Scholer, M., and D. Burgess, The role of upstream waves in supercritical quasi-parallel shock reformation, *J. Geophys. Res.*, **97**, 8319-8326, 1992.

Figure 1. ISEE-3 and GEOTAIL orbits during the periods on the GSE-XY plane, between 23 September and 1 October, 1983, and between 4 and 10 August, 1993, respectively. The XZ projection (panel a, top) and the XY projection (panel b, bottom) are shown. Stars show the positions at 00 UT of each day. A dashed curve in panel b shows the nominal bow shock surface.

Figure 2. ISEE-3 observation of the magnetic field. The intensity B , the latitudinal angle θ , the azimuthal angle ϕ , the normalized fluctuation amplitude (see text) are shown from the top.

Figure 3. GEOTAIL observation of the magnetic field with the same format as Fig. 2.

Figure 4. The power spectrum of the magnetic field fluctuation perpendicular to the averaged field direction. (The spectrum is calculated from 1800 point Fourier transformation with 5 degrees of freedom.) Observation was made between 1:39 and 1:48 UT on 6 August, 1993. The dot line is proton cyclotron frequency.

Figure 5. Panels a and b show the normalized amplitudes of the upstream transverse magnetic field fluctuation observed by ISEE-3 (top) and GEOTAIL (middle), respectively. Panel c (bottom) shows the distances D from the nominal bow shock surface to the spacecraft. The curves in panels a and b are the result of the exponential function fitting (see text).

Table 1a. Solar wind parameters for the ISEE-3
upstream interval

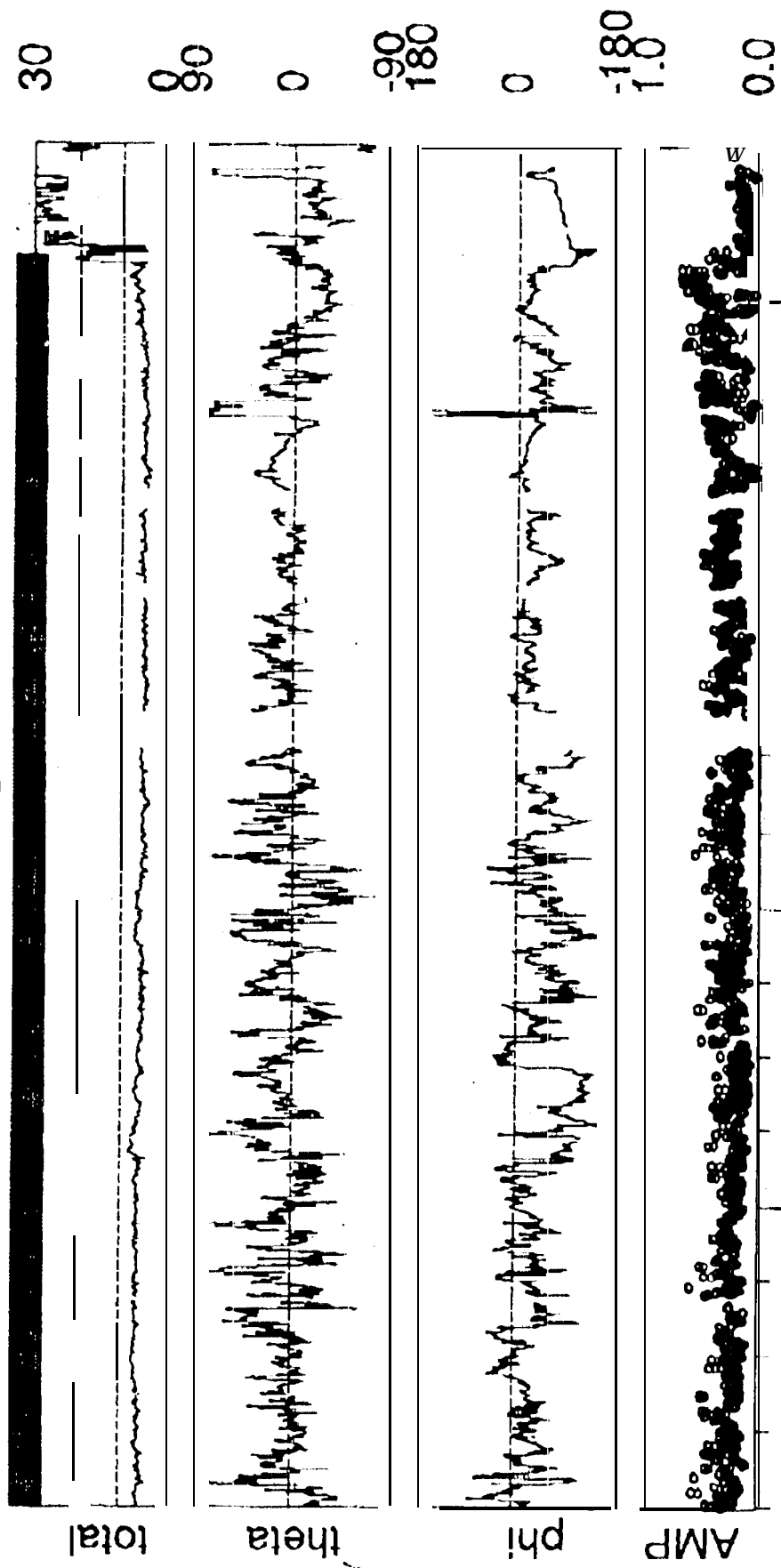
date	velocity	density	magnetic	M_A
yyymmdd (km/s)	(1/cm ³)	field (nT)		
830927	510-630	2-4	6-7	6-7
830928	480-500	3-6	6-7	6-8
830929	420-460	2-5	6-6	8-9
830930	350-390	2-b	5-6	4-7

Table 1b. Solar wind parameters for the
GEOTAIL upstream interval

date	velocity	density	magnetic	M_A
yyymmdd (km/s)	(1/cm ³)	field (nT)		
930806	421-465	8-15	7-8	8.11
930807	387-438	7-13	7	7-11
930808	462-303	3-8	5-7	6-11
990809	468-487	6-9	7	"(-1 u

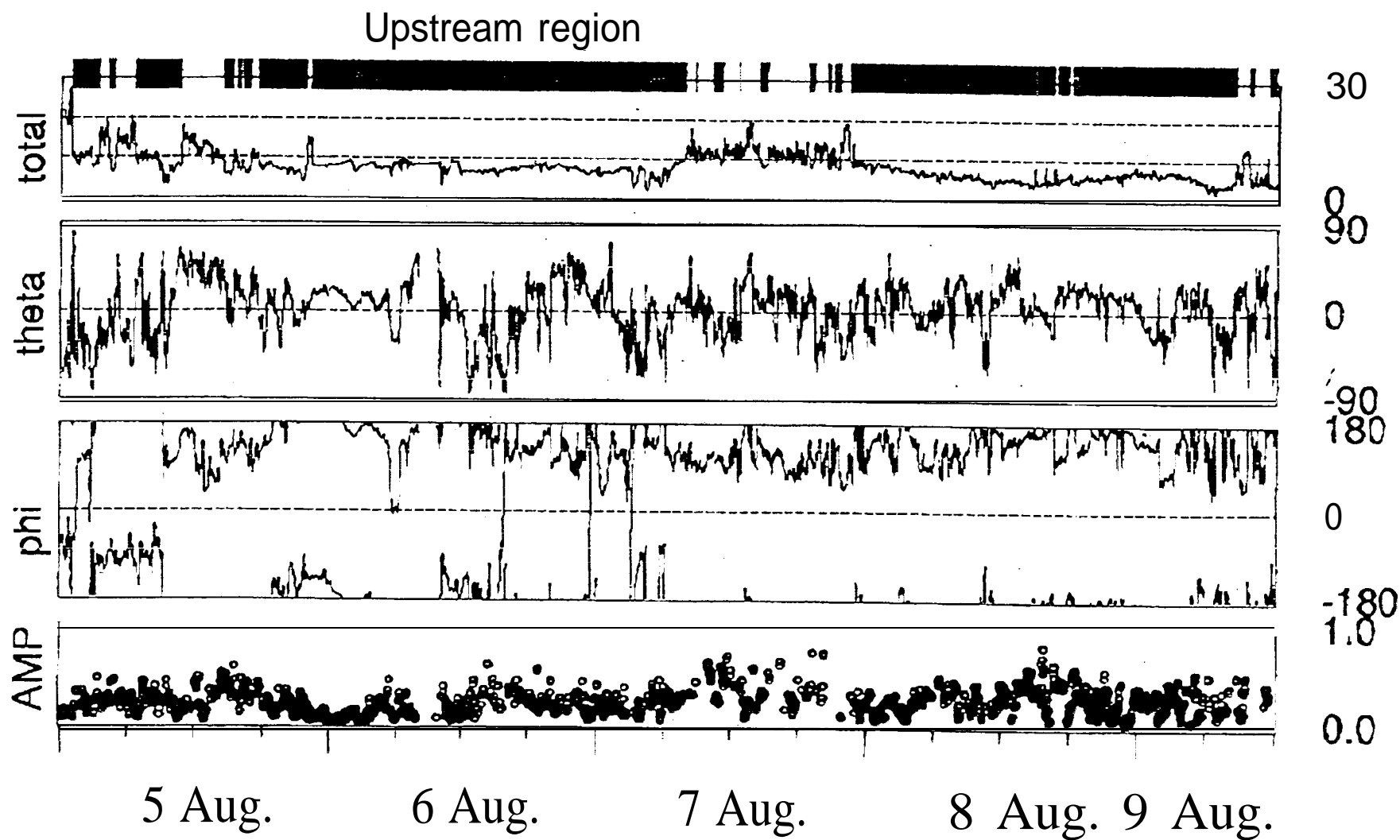
ISEE - 3 Magnetic Field 1983

Upstream region



27 Sep. 28^{CA} Sep. 29 Sep. 30 Sep. 1 Oct.

GEOTAIL Magnetic Field 1993



Spectrum

6.Aug 1993. 1:39~1.48

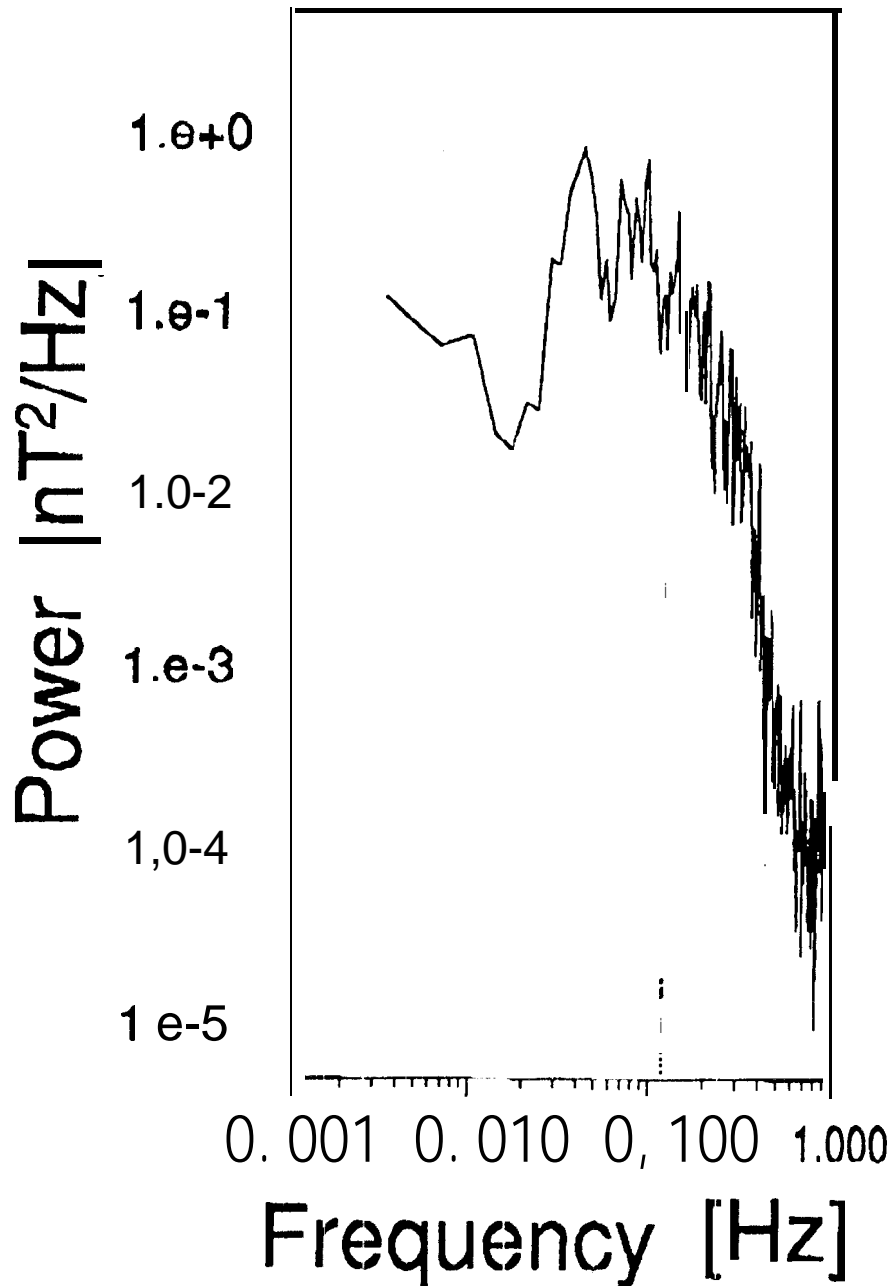


Fig. 4

